A revised alpha-ejection correction calculation for (U-Th)/He thermochronology dates of broken apatite crystals

John J. Y. He[1], Peter W. Reiners[1,2]

[1]Department of Geoscience, University of Arizona, Tucson, AZ, 85721, USA

5 [2]Faculty of the Environment, University of Northern British Columbia, Prince George, BC V2N 4Z9, Canada

Correspondence to: John He (johnhe@email.arizona.edu)

Abstract. Accurate corrections for the effects of alpha ejection (the loss of daughter He near grain or crystal surfaces due to long alpha-stopping distances) is central to (U-Th)/He thermochronometry. In the

10 case of apatite (U-Th)/He dating, alpha-ejection correction is complicated by the fact that crystals are often broken perpendicular to the c-axis. In such cases the correction should account for the fact that only some parts of the crystal are affected by alpha-ejection. A common current practice to account for such broken crystals is to modify measured lengths of broken crystals missing one termination by a factor of 1.5, and those missing both terminations by a factor of 2. This alpha-ejection "correction correction"

15 systematically overestimates the actual fraction of helium lost to alpha ejection, and thus overcorrects the measured date relative to that determined for an otherwise equivalent unbroken crystal. The alpha-ejection-affected surface-area-to-volume ratio of a fragmented crystal is equivalent to the surface-area-to-volume ratio of an unbroken crystal twice as long (for fragments with one termination), and equivalent to that of an unbroken crystal infinitely long (for fragments with no termination). We suggest it is

20 appropriate to revise the fragmentation correction to multiply the length of crystals missing one c-axis termination by 2, and those missing both c-axis termination by some large number >~20, respectively. We examine the effect of this revised correction and demonstrate the accuracy of the new method using synthetic datasets. Taking into account alpha-ejection, rounding of the He concentration profile due to diffusive loss, and accumulation of radiation damage over a range of thermal histories, we show that the

25 revised fragmentation alpha-ejection correction proposed here accurately approximates the corrected date of an unbroken crystal ("true" date) to within < 0.7% on average (±4.2%, 1σ), whereas the former method overcorrects dates to be ~3% older than the "true" date, on average. For individual grains, the former method can result in older dates by a few percent in most cases, and by as much as 12% for grains with aspect ratio of up to 1:1. The revised alpha-ejection correction proposed here is both more accurate and

30 more precise than the previous correction, and does not introduce any significant systematic bias to the apparent dates from a sample.

1 Introduction

Since the development of modern apatite (U-Th)/He thermochronometry, the technique has become a versatile and powerful tool for a range of geological problems (Zeitler et al. 1987; Farley *et al.,* 1996; Flowers et al., 2022 a, b). To fully leverage the power of the technique, however, it is necessary to account for the wide range of possible complications that commonly cause data dispersion greater than analytical errors. Of particular significance is correcting for the loss of daughter nuclides due to the problem of alpha ejection. Apatite He dating uses the accumulation of daughter nuclide ^{4}He (i.e., alpha particles) from the spontaneous alpha decay of ^{238}U, ^{235}U, and ^{232}Th (as well as a minor contribution from ^{147}Sm) to constrain possible thermal histories of samples, which is sometimes simplified as providing a date of cooling through some closure temperature (~30-90 °C) at which helium diffusion out of a crystal is sufficiently slow for the system to be considered closed. However, this method is complicated by the fact that the sizes of most typical apatite crystals are only several times greater than the stopping distance of alpha particles (~20 μm), meaning that the fraction of ^{4}He ejected from a crystal must be accounted for in most applications (Farley *et al.,* 1996).

Careful measurement of crystal geometries allows accurate approximation of the cumulative alpha-ejection loss of helium from a crystal (Ziegler; 1977; Farley *et al.,* 1996; Farley, 2002; Hourigan et al. 2005; Ketcham et al. 2011; Reiners *et al.,* 2018). Because the likelihood of an alpha particle being ejected from a crystal is directly related to a parent nuclide's proximity to the crystal surface, the fraction of helium retained in the crystal (F_T) is a function of a crystal's surface area to volume ratio (β) (Farley *et al.,* 1996). In the simplest case of a spherical grain with homogenous parent nuclide distribution, F_T is a cubic polynomial function of β (Farley *et al.,* 1996). F_T can be estimated for other geometries using a polynomial function calibrated by Monte Carlo alpha-ejection models (Farley, 2002; Ketcham et al, 2011). In practice, a parent-nuclide-specific F_T^i is determined and a corrected date can be calculated by incorporating it into the full decay equation:

$$^4He = 8(^{238}U)(F_T^{238})\left(e^{\lambda_{238}t} - 1\right) + 7(^{235}U)(F_T^{235})\left(e^{\lambda_{235}t} - 1\right) + 6(^{232}Th)(F_T^{232})\left(e^{\lambda_{232}t} - 1\right)$$
$$+ (^{147}Sm)(F_T^{147})\left(e^{\lambda_{147}t} - 1\right)$$

[Eq. 1]

where t is the unknown variable that must be solved numerically or iteratively; ^{4}He, ^{238}U, ^{235}U, ^{232}Th, and ^{147}Sm contents are measured; λ_i is the decay constant for the given isotope; F_T^i, the alpha-ejection correction factor for the given isotope calculated from crystal geometry (Ketcham *et al.,* 2011). A more approximate corrected date can also be calculated by simply dividing the measured (raw) date by F_T (Farley and Stockli*,* 2002), though this is less accurate for older dates.

65 These calculations generally assume the ideal case of a euhedral, prismatic crystal with homogenous parent nuclide distribution, entire original crystal faces, and insignificant parent nuclide concentrations outside and within one alpha-stopping distance of the exterior of the crystal during the interval in which temperature was low enough to accumulate He. When these assumptions are violated, further adjustments to the standard F_T correction are required.

70 If information about the magnitude and pattern of parent-nuclide zonation is available, an adjusted F_T may be applied to account for inhomogeneous parent-nuclide distribution (Hourigan *et al.,* 2005, Farley *et al.,* 2011, Ault and Flowers, 2012, Gautheron et al., 2012). Absent such information, as is the case in most routine analyses, use of the standard unzoned correction assuming homogenous distribution of the parent nuclide would introduce errors that skew a crystal's apparent date to be younger, if its rim is

75 enriched in parent nuclides, and older if it is depleted in parent nuclides (Farley et al., 1996; Hourigan *et al.,* 2005). For apatite, these errors are usually minor (<1.5% for 80% of apatite crystals, and <9.5% for 95%), because apatite crystals in most cases do not typically exhibit extreme zonation of parent nuclides (Ault and Flowers, 2011, in the case of old cratonic samples). The data from that study suggests that the errors are usually symmetrically distributed, with apatite populations not exhibiting bias towards either

80 rim-enriched or rim-depleted grains, though this may not be the case for rocks that experienced metamorphism or hydrothermal alteration. Accounting for effects of He implantation from sources external to the grains is not typically possible for grains separated from their petrographic context, although in some cases particular date-eU (effective uranium concentration) or date-Rs (sphere-equivalent radius) correlations may be used to interpret such effects (Spiegel et al., 2009; Murray et al.,

85 2014).

The focus of this paper is the adjustment to the F_T correction that should be made in the case of crystals that are broken perpendicular to the c-axis, as common for apatite, whether during mineral separation or during erosion and transport (if the fragmentation post-dated cooling). If errors due to fragmentation are large, they can significantly impede our ability to extract geologically meaningful information from dates

90 calculated from parent-daughter nuclide ratios. Broken and morphologically suboptimal crystals are frequently analyzed, particularly when the quality of mineral separates is poor and/or the apatite yield from a sample is low. In addition, imperfect basal (0001) cleavage in apatite (Dana, 1963; Palache et al., 1963) leads to the fact that many dated crystals are broken perpendicular to their c-axis and lack original terminations, even for high-quality samples. A common strategy is to apply a fragmentation correction to

95 the F_T calculation, which accounts for the fact that the fracture exposes surface area where alpha ejection did not occur (Farley, 2002). This correction seeks to approximately correct for the originally greater length of the unbroken apatite crystal, by multiplying the length of all broken crystals by 1.5 (if one end is broken) or 2 (if both ends are broken) (Farley, 2002; Farley *et al.,* 1996; Brown *et al.,* 2013; Beucher et al., 2013; Reiners *et al.,* 2018). Though it is not possible to find the original length of broken crystals,

100 Farley (2002) argued that these approximations are sufficient because F_T is relatively insensitive to the length of the crystal.

An alternative approach to this problem is that of Brown et al. (2013), who argued that, for interpreting thermal histories, it is best to leave dates uncorrected and instead evaluate the variation in date among crystals with different morphologies and numbers of broken ends. If one assumes that breakage occurred

105 prior to cooling to temperatures of partial He retention, raw (uncorrected) dates of broken crystals can vary by up to 60% for certain t-T histories, and that for sufficiently large datasets of fragmented crystals, considering the patterns of dispersion in uncorrected dates can constrain thermal history (Brown et al. 2013). In practice, however, F_T-corrected dates remain widely reported, partly because correcting for alpha ejection and fragmentation is necessary to compare dates to other datasets and dates of geologic

110 significance. A more accurate correction would allow both broken and unbroken crystals within a sample and across samples to be appropriately compared without introducing additional systematic bias.

Although the conventional fragmentation correction has been widely applied, its accuracy and precision has not been demonstrated. In the first part of this paper, we consider the rationale behind the early approach, then propose a revision and compare the results of both methods. We test the new method using

115 synthetic data and demonstrate the accuracy of the revised correction. We take into account a range of broken crystal sizes, number of terminations present, and various thermal histories and their associated effects on helium diffusivity, and we quantify the uncertainty that can be attributed to the fragmentation correction alone. Considering the numerous natural sources of uncertainty in apatite He dating, achieving greater confidence in the accuracy of the fragmentation F_T correction and minimizing its uncertainty

120 ultimately aids in the interpretation of other possible sources of uncertainty and errors (He et al., 2021).

2. Revision of F_T correction for broken crystals

For an idealized spherical grain, the alpha-ejection correction is a function of the radius of the sphere (R) and the alpha stopping distance for the given parent nuclide (S):

125
$$F_T = 1 - \frac{3S}{4R} + \frac{S^3}{16\,R^3}$$

[Eq. 2]

(Farley et al., 1996). Where $R>>S$, the function approaches a linear relationship:

$$F_T = 1 - \frac{3S}{4R} \quad \text{or}, \quad F_T = 1 - \frac{S\beta}{4}$$

[Eq. 3]

130   (Farley et al., 1996), where β is the ratio of surface area of a crystal to its volume. In other words, the fraction of helium lost due to alpha ejection near the crystal surface is approximately a function of the ratio of surface area of a crystal to its volume. Considering more realistic crystal geometries, polynomial equations that define the F_T^i value as a function of β have been empirically determined using Monte Carlo simulations for each parent nuclide i and their respective alpha stopping distance (Farley et al., 1996;

135   Hourigan et al., 2005). For hexagonal prisms, simply measuring the length (L) and radius or half-width of the cylindrical prism (R) allows the computation of β:

$$\beta = \frac{2R + (4/\sqrt{3})L}{LR}$$

[Eq. 4]

The general idea behind modified F_T corrections is to modify β, under the assumption that the polynomial

140   functions relating β and F_T are nearly identical for similar geometries (e.g., hexagonal prism with bipyramidal or pinacoidal terminations). This was the approach taken to correct for lost crystal surface in the case of crystals polished parallel to the c-axis (Reiners et al., 2007). In the case of c-axis perpendicular breakage, the Farley et al. (1996) approach sought to establish the length of the original, unbroken crystal. Because it was observed that the corrected-length-to-radius ratios of most apatite crystals (5:1) were

145   sufficiently high such that the F_T corrections become largely independent of length, it became standard practice at most laboratories to simply modify β by multiplying the lengths of broken crystals by arbitrary factors of 1.5 or 2, thereby modifying F_T (Farley *et al.* 1996; Farley, 2002). Alternatively, in the slightly different context of inverse modelling a large set of uncorrected ages, Beucher et al. (2013) suggested that a rule of thumb for predicting the unknown initial length should be to add the maximum fragment

150   length of a set of fragments and two times the maximum radius. To the first order, guessing the unknown initial length using consistent factors such as these suffices to roughly account for the loss of alpha-ejection-affected surface area at the tips: this is because as L increases, the increase in surface area of a crystal is less than that of the volume, in effect reducing β.

In detail, however, the fraction of helium remaining in a fragmented crystal does not depend on the

155   unknown (and precisely unknowable) initial length. Rather, it should be directly related to the surface area of a broken crystal that was originally affected by alpha-ejection. Assuming that we can identify when crystals have lost one or both terminations, that the breakage generally occurs more than one average-alpha-stopping-distance from the tip, and that diffusion has not significantly modified the daughter concentration profiles, the alpha-ejection-affected-surface-area-to-volume ratio ($β_α$) could be

160   simply calculated by measuring and then subtracting the surface area of the broken face(s) from the total surface area. For a hexagonal prism, simple geometric calculations demonstrate that the $β_α$ of singly and doubly broken crystals are equivalent to the β of an unbroken crystal of the same width that is twice as

long, or infinitely long, respectively; this is shown graphically in Fig. 1. Consider that the helium profile in an unbroken crystal is symmetrical such that when broken in half, each half will have the same fraction of helium remaining (F_T); thus, conversely, any broken crystal with one termination (breakage occurring more than one alpha-stopping distance from the tip) has the same F_T as a hypothetical unbroken crystal double its length. For crystals with no terminations remaining, any c-axis perpendicular segment or cross section of the crystal will have the same F_T, no matter its length or its position along the fragment; therefore fragments with no terminations have the same F_T as an infinitely long unbroken crystal, where the terminations, which have a different F_T, have a vanishingly small effect on the overall F_T of the crystal.
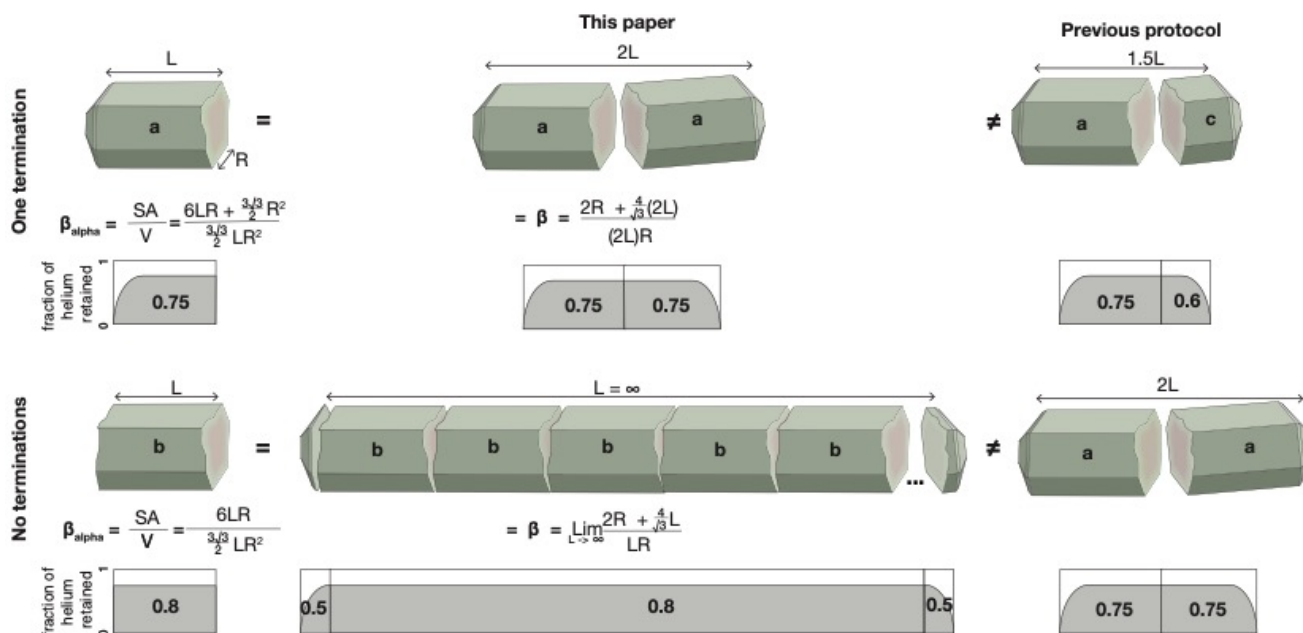
Fig. 1. The alpha-ejection-affected surface-area-to-volume ratio, or β_α, of a broken crystal that has lost a basal fragment longer than one alpha-stopping distance is equivalent to the surface-area-to-volume ratio of an unbroken crystal twice as long (for fragments with one termination), and equivalent to that of an unbroken crystal infinitely long (for fragments with no termination). The simple geometric calculations shown assume a flat hexagonal termination, but apply by the same logic to any geometry, regardless of the shape of its body (e.g. cylindrical, tetragonal, or hexagonal) or the shape of its terminations (e.g. pyramidal, flat, or rounded). The profiles of fraction of helium retained that are shown below each fragment are schematic and serve only to illustrate the equivalence or non-equivalence of fragments of different lengths (e.g. a = 0.75, b = 0.8, c = 0.75), and do not correspond to any specific dimensions. As discussed in text, these calculations assume no change to the daughter concentration profile due to diffusion.

It follows, then, that a more accurate fragmentation correction that explicitly considers the lost surface area of a broken crystal should be to multiply the length of a broken crystal by 2 or some large number (to simulate the limit as L approaches infinity), respectively, rather than 1.5 or 2, i.e.:

185    $\beta_a = \dfrac{2R + (8/\sqrt{3})L}{2LR}$ for crystals broken on one end; and

[Eq. 5]

$\beta_a = \lim\limits_{L \to \infty} \dfrac{2R + (4/\sqrt{3})L}{LR}$ for crystals broken on both end

[Eq. 6]

where L is the measurement of the crystal dimension perpendicular to the fracture (since crystals
190   commonly break perpendicular to the c-axis in apatite crystals, L should usually be measured parallel to
the c-axis, even if it is shorter than the width). In the unlikely case of an oblique fragment, L should be
the average of the longer and shorter sides. This simple correction has the benefit of applying to other
geometries, regardless of the shape of its body (e.g. cylindrical, tetragonal, or hexagonal) or the shape of
its terminations (e.g. pyramidal, flat, or rounded): the β_α of any singly broken crystal is equivalent to the
195   β of a whole crystal twice its length, and the β_α of any doubly broken crystal is equivalent to the β of a
whole crystal infinitely long. The correction can thus be applied to all crystals broken perpendicular to
the c-axis, regardless of original length, requiring knowledge of only the width and length of the broken
crystal, and the number of terminations present. Similarly, this correction can be applied to zircon
fragments, using the appropriate beta equation (though it is less common to see zircon fragments with
200   only one termination or no terminations). We emphasize that though this fragmentation correction is
similar in form to that of Farley (2002) in that it involves length-modifying factors, it differs in that it
seeks to approximate the length of a whole crystal with the same fraction of helium remaining as the
fraction remaining in the broken fragment, rather than seeking to approximate the unknown length of the
original unbroken crystal.

205
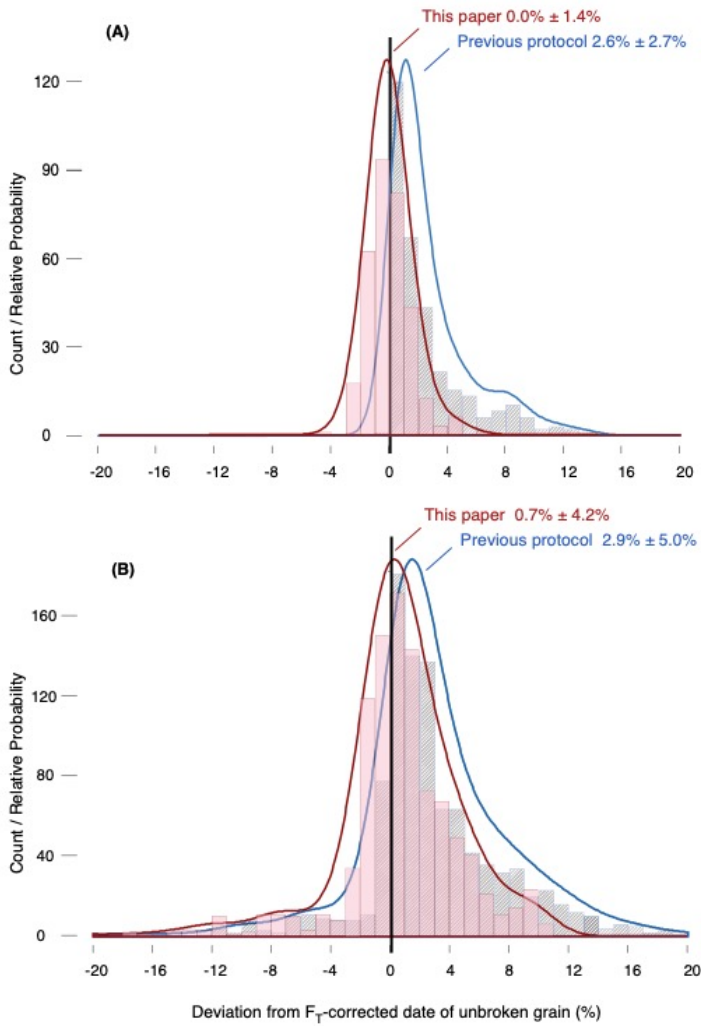
Fig. 2. Histograms and kernel density estimate (KDE) functions comparing the new protocol suggested in this paper (red) and the previous protocol (blue), as applied to a synthetic dataset of raw, uncorrected dates (n=1000, cf. Brown et al., 2013). The error is defined to be the % deviation of the F_T-corrected dates of a broken crystal from the F_T-corrected date of the whole crystal, which is known because the synthetic fragments are generated from a whole crystal with a known "age". The new protocol is more accurate and more precise at correcting for the effect of fragmentation, both in the ideal case (A) assuming that fragmentation has occurred more than one average-alpha-stopping-distance from the tip, and that there is no significant diffusive modification of the helium profile, as well as in the more realistic scenario (B), which includes corrected dates from fragments that are broken close to the tip, and fragments that experienced thermal histories leading to significant diffusive modification, in addition to the dates contained in (A). Annotations show the mean ± standard deviation (1σ); KDE functions are normalized to the same peak height.

3. Accuracy and precision of the revised F_T correction

To characterize the uncertainty of the new and old protocols, we applied the above fragmentation correction equations to a synthetic dataset of raw (uncorrected) dates of broken prismatic crystals where the corrected dates of the original unbroken crystals are known. Note that as a simplification, a length-modifying factor of 20 is used to approximate the limit to infinity (see Section 4.1). For comparable results between the new and old protocol, we used the same datasets of raw uncorrected dates from Brown *et al.* (2013), which are generated from the volume-integrated [4]He concentration in a random set of crystal fragments broken at varying positions along the original crystal (Beucher *et al.* 2013). We assume uniform spatial distribution of the parent nuclide, and apply both protocols to all fragments exactly as we would calculate F_T corrected dates in routine laboratory analyses: i.e. we assume no knowledge of the original length and thermal history of the crystals to compute the corrected age, and use only the raw date, length and width of the broken crystals, and the number of terminations present for the calculation. We then compare the F_T-corrected dates of the synthetic fragments with the known F_T-corrected date of the corresponding unbroken crystals. These original unbroken crystals from which the fragments were generated have a constant geometry (hexagonal prism that is 400 μm long and 150 μm wide), and experienced one of five different representative thermal histories (rapid monotonic cooling; slow monotonic cooling; prolonged isothermal residence in the partial retention zone followed by rapid cooling; a mix of slow cooling and isothermal holding in the partial retention zone; and gradual reheating (e.g. burial) followed by rapid cooling; cf. Wolf *et al.* 1998).

To test the accuracy of the proposed protocol under the stated ideal assumptions (that the fragmentation has occurred more than one average-alpha-stopping-distance from the tip, and that there is no significant diffusion-induced modification of the helium concentration profile), we excluded any randomly generated crystals broken <20 μm from the tip, and included only fragment sets that experienced the two thermal histories (monotonic cooling) associated with the least amount of diffusive modification of the helium profile (Fig. 2a). To approximate the actual circumstances under which fragments are analyzed in laboratories, where we have no a priori knowledge of the thermal history and cannot readily discern where a crystal has broken, we included the full fragment dataset (Fig. 2b). 23% of the randomly generated fragments in that dataset were broken within ~20μm from the tip, and 60% experienced complex thermal histories involving reheating or extended residence in the partial retention zone.

The new protocol accurately corrects for the effect of fragmentation, deviating by 0.0% ± 1.4% (1σ) from the corrected date of the unbroken crystal, under the ideal assumptions stated above (Fig. 2a). By comparison, under the same assumptions, the old protocol leads to corrected dates that are almost all too old, on average by 2.6% ± 2.7%. When the two assumptions are not met, the proposed fragmentation correction results in a broader range of uncertainty (+0.7% ± 4.2%), but it is nevertheless more accurate

and more precise than the old protocol (+2.9% ± 5.0%) (Fig. 2b). Using the new protocol, only 3% of corrected dates deviate from the corrected date of the unbroken crystal by greater than 10%; this represents a 66% reduction relative to the prior protocol.

255
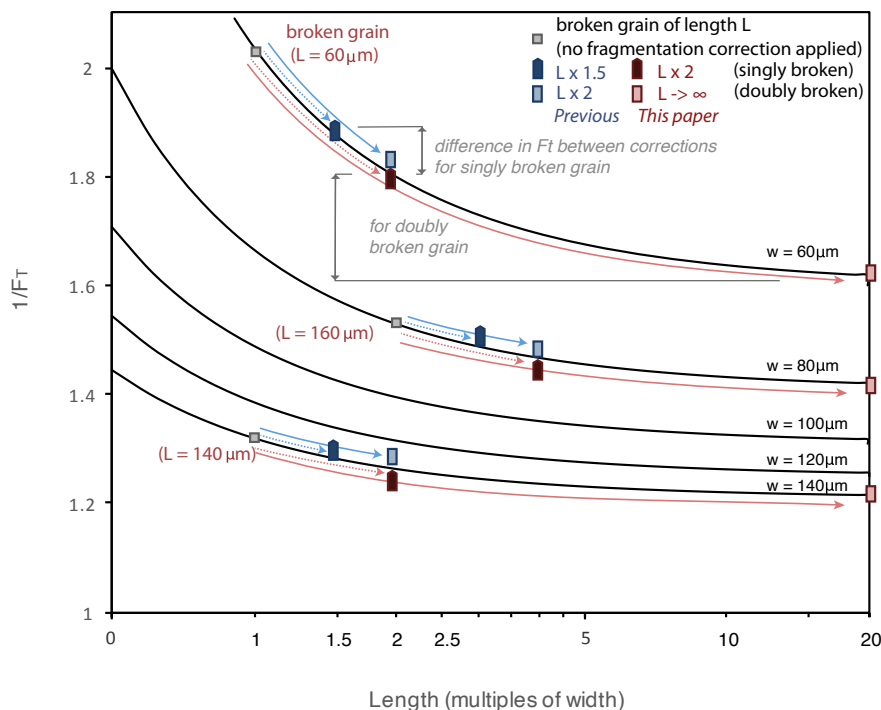
Fig. 3. The inverse of F_T value plotted as a function of crystal length L, as used in the calculation of β or β$_α$. For a broken crystal, this is measured parallel to the c-axis (as a multiple of width), and modified by some factor (see legend). The inverse of F_T can be
260 approximately considered a multiplier for the raw date, where corrected date ≈ raw date x (1/ F_T) (Farley et al., 1996). Inverse F_T corrections for three example fragments are shown (width = 60, 80, and 140μm, and length = 60, 160, and 140, respectively), with the corresponding fragment-corrected F_T values for singly- or doubly-broken crystals. The gray squares indicate the actual length of the fragment, and show their inverse F_T values if no fragmentation correction is applied. For convenience, the asymptotic value is assumed to be approximately the same as multiplying by some large number (e.g., 20). Note that strictly speaking, calculation of
265 a corrected date requires using the full decay equation with an individual F_T^i for each nuclide, rather than the simplification of corrected date ≈ raw date*(1/ F_T).

4. Discussion

4.1. Difference between corrections for different crystal dimensions

Though multiplying a fragment length by different factors may seem to be a minor revision, the resulting difference in corrected dates is not negligible. This is partly because the observation that F_T corrections is not strongly dependent on length, upon which the fragmentation correction was initially based, does not hold true for the smaller crystals commonly analyzed today (e.g., c-axis perpendicular width < 150μm). Fig. 3 shows the effect of crystal length (or modified crystal length, as used in the calculation of β or $β_α$) on the inverse value of F_T, an approximation for the correction's effect on the final reported date (Fig. 3). Since both protocols effectively multiply the length of a broken crystal to compute an adjusted F_T value, the inverse F_T values of the new and old protocols for any given crystal width all lie on the same curve for F_T as a function of length (normalized to width). Particularly when the length of a broken crystal is close to its width, and when the width is small, the F_T correction is not independent of the modified length. For example, for a singly-broken crystal that is 60 μm in width and equally long (the minimum dimensions of crystals routinely analyzed in our lab), the difference between the new and old protocols, would be 4%; for a doubly-broken crystal of the same dimensions, the difference would be 12% (Fig. 4). The overcorrection of the previous protocol could be even larger for drum-shaped fragments (i.e. crystals broken on both ends, and shorter in c-axis-parallel length than width). For a broken crystal that is 140 μm in both width and length, the difference would be 2% and 5% (for singly and doubly-broken crystals, respectively). The magnitude of these differences is not negligible, at least relative to other sources of error in F_T corrections. By comparison, for example, the updated alpha-ejection models of Ketcham *et al.* (2011) based on revised alpha-stopping distances affects dates by approximately 1-5%, and 2D measurement of crystal geometry introduces errors of ~2% (Cooperdock et al., 2019).
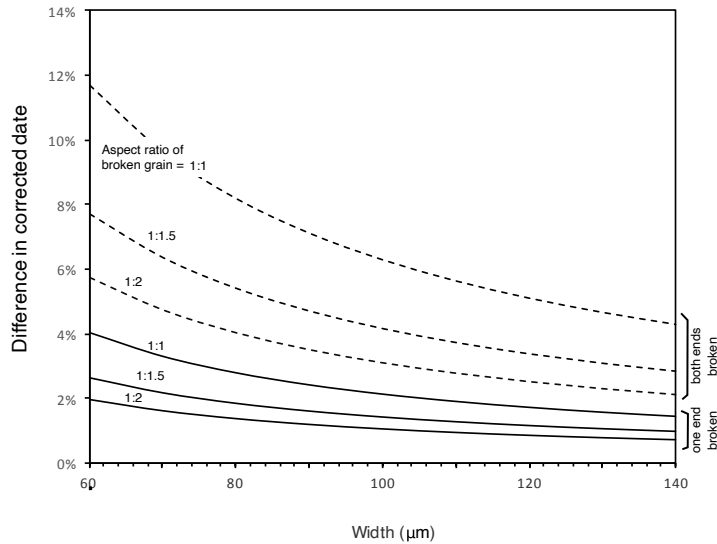
Fig. 4. Difference between the corrected date calculated from the standard protocol and revised protocol (Dashed—broken on both ends; Solid—broken on one end), shown for a range width-to-length ratios commonly seen in broken crystals.

4.2. Uncertainty in fragmentation correction compared to other sources of date dispersion

In the ideal case (that the fragmentation has occurred more than one average-alpha-stopping-distance from the tip, and that there is no significant diffusion-induced modification of the helium concentration profile), we have shown that the proposed fragmentation correction is both accurate and precise (+/-<1.4%). When these ideal assumptions are not met, the uncertainty increases (+/-4.2%) (Fig. 2b). The larger uncertainties are largely due to the diffusive modification of helium profiles. In our test of this protocol, all cases of corrected fragment dates that deviate by more than >5% from the corrected date of the unbroken crystal can be attributable to thermal histories involving prolonged residence in the partial retention zone (Fig. 5). Without a priori knowledge of a sample's thermal history, this is a problem for the new fragmentation correction just as it is for the old protocol, because the calculation of F_T correction only assumes loss of helium due to alpha ejection. The additional uncertainty associated with the fragmentation correction fundamentally relates to the fact that using β_α to correct F_T implies taking the

310   lost surface area ("skin") affected by alpha ejection as a proxy for the lost volume (the outer "shell") of
the crystal affected by alpha ejection.
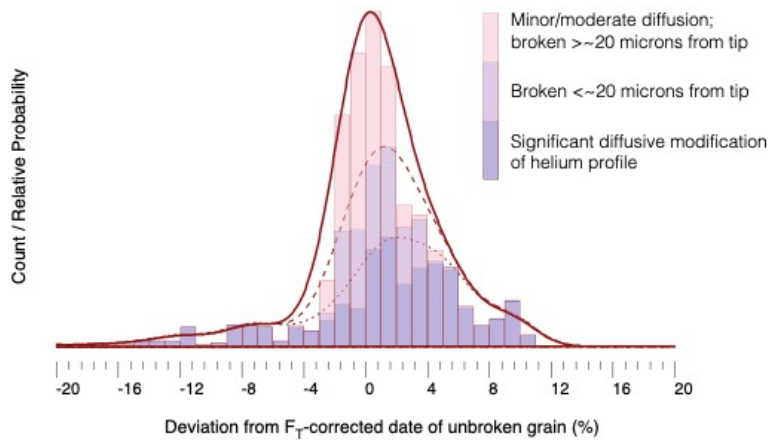
Fig. 5. Uncertainty associated with the proposed fragmentation correction due to inclusion of fragments broken too close to the tip (dashed) and due to thermal histories that involve significant diffusive modification of the helium profile (dotted). The histogram
315   **and curves are stacked and cumulative, such that the dashed probability curve includes both close-to-tip fragments as well as fragments with significant diffusive loss.**

We emphasize that because the F_T-corrected dates of the fragments are compared to the F_T-corrected date of a whole crystal, Fig. 2 and Fig. 5 assesses only the effect of brokenness correction alone. Parent-nuclide
320   zonation, eU variation, and diffusive helium loss remain important sources of additional error and dispersion (e.g. Meesters and Dunai, 2002; Herman et al., 2007, Gautheron et al 2012, Brown et al., 2013; Beucher et al., 2013). Notwithstanding the effects of date variation due to all these effects, the fragmentation correction proposed in this paper more consistently and accurately reproduces the F_T-corrected date of unbroken crystal. An illustrative case is that of a hypothetical date-elevation transect
325   from a crustal block that cooled slowly through the partial retention zone until some point in time, then subsequently experienced very rapid cooling (from Brown et al., 2013). A key observation of Brown et al. (2013) was that the large dispersion of raw uncorrected fragment dates is due to the fact that these dates can be both younger and older than the whole crystal, and that fragments of same length can yield different dates, while conversely, fragments of different lengths can yield the same date. The dispersion
330   is compounded because slow cooling leads to significant diffusive modification of the helium profile in a crystal. Despite this large dispersion of uncorrected fragment dates (up to 60%), and despite variations in eU and grain sizes, applying the new fragmentation correction introduces limited uncertainty relative to the dispersion caused by other effects (Fig. 6). This facilitates interpretation of widely-dispersed data

by reducing the number of variables that must be considered, and demonstrates the utility of applying a
335 fragmentation correction when analysis of the pattern of dispersion in >20-30 crystals is not practical.
Finally, while both the new and old F_T correction for broken crystals reliably approximates the corrected
date of an unbroken crystal for a range of eU and crystal sizes, the new correction reduces the systematic
bias that is introduced by the old protocol when many broken crystals are analyzed in a sample by ~3-4%
(Fig. 6).

340
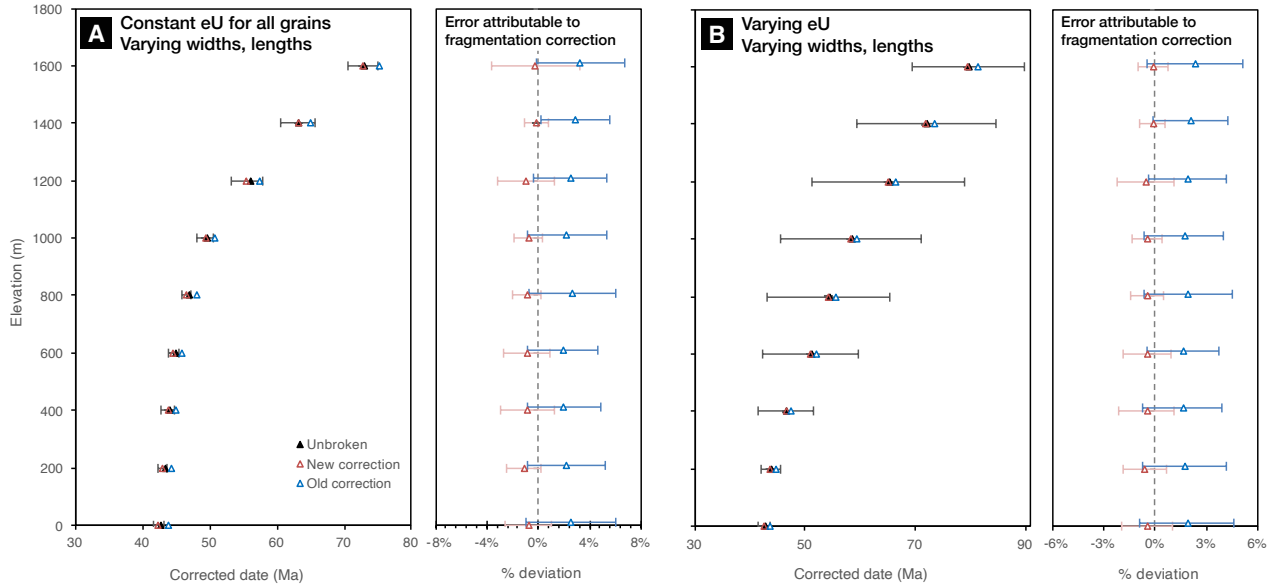
Fig. 6. a) Date-elevation transect of a crustal block that cooled slowly through the partially retention zone, and was subsequently rapidly exhumed (cf. Brown et al. 2013, Fig. 9), showing fragment dates corrected using the new protocol (red), compared to previous protocol (blue), and the expected whole-crystal date (black). Note that the red and black triangles may be difficult to distinguish
345 **because they overlap in most cases. Corrected dates are from fragments of varying lengths, both singly and doubly broken, generated from crystals with variable widths and lengths, but constant eU. Error bars in date-elevation transect represent intra-sample date dispersion and are shown for the new protocol only. Error bars in the right panel show the % deviation of the corrected fragment dates from their corresponding corrected whole-crystal dates, using the new (red) and old protocol (blue). (b) Same as (a), but fragments were generated from crystals of varying eU (15-100 ppm, Brown et al., 2013), in addition to varying width and length.**
350 **Notice that the introduction of eU as a variable significantly increased the intra-sample dispersion of corrected dates, but that the error attributable to the fragmentation correction alone was not materially affected. All error bars are 1σ.**

Ultimately, the characterization of the uncertainty due to the application of the fragmentation correction
moves us one step closer to a more comprehensive quantification of all the uncertainty involved with
355 apatite He dating (Fig.7). Previous work has already shown, for example, that

(1) size- and eU-dependent diffusivity can cause apparent dates to systematically vary (Reiners and Farley, 2001; Flowers et al. 2009; Whipp et al., 2022).

(2) The presence of extraneous daughter nuclides whose parent nuclides are not accounted for can cause outlier dates many multiples older than the true date (^{4}He-rich fluid inclusions; U- or Th-rich inclusions or microinclusions where the inclusions are not fully dissolved; grain boundary phases or adjacent grains that contribute helium to the grain but are not in the analyzed aliquot) (Spiegel et al. 2009; Fitzgerald et al. 2006; Murray et al. 2014).

(3) Non-uniform distribution of the parent nuclides (i.e., "zonation") can cause dates to be both older or younger by <1.5% in most cases. Even if zonations are not accounted for, the probability distribution of errors due to zonations can be approximated by either examining a representative selection of apatite in a sample, or using a reference compilation (e.g. Ault and Flowers, 2011) (Fig. 7a).

(4) Technician-to-technician differences in 2D grain measurement cause date variations that differ from actual 3D geometry by ~2%. (Cooperdock et al., 2019)

A future step towards a more rigorous evaluation of the uncertainty of individual-grain analyses or samples as a whole could involve the propagation of each of these uncertainties to account for sample and grain specific information such as the probability of implantation (approximated from the spatial distribution of heavy minerals in a sample, via X-Ray Computed Tomography), the probability of extreme parent nuclide zonations in a sample (based on fission track mounts) or from a reference compilation, and whether fragments were analyzed. The resulting distribution (e.g. Fig. 7d) would then represent the sample-specific probability of single-aliquot apatite He dates. For larger datasets, especially in the case of larger-n analyses (e.g. Fig. 7e), this would provide a more robust rationale for the interpretation of the geologically significant date. For smaller datasets, the expected distribution would inform our selection of the appropriate summary statistic to represent the date variation in a given sample (He et al., 2021).
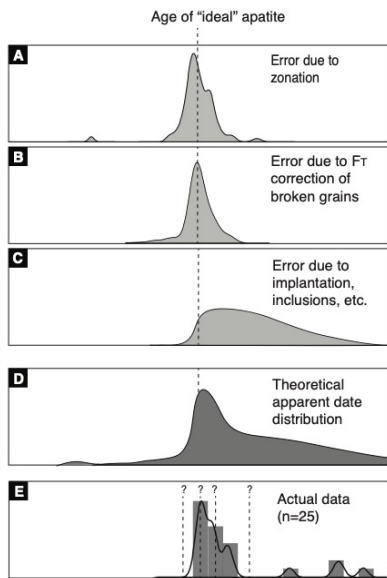
Fig. 7. Illustration of how uncertainties due to different complications in apatite helium dating, e.g. uncertainty due to zonation (a), uncertainty due correction for broken crystals (b), and error due to implantation and other effects (c) could together be combined to form a theoretical apparent date distribution (d) that would inform our interpretation of real data and the choice of the appropriate summary statistic (whether the minimum, mean, median, peak date) in representing a sample's date. Note that (a) is based on actual data from Ault and Flowers (2011), (b) is based on this study, whereas (c) is schematic. The last panel (e) is a representative sample (n=25) that shows the expected non-normal and right-skewed distribution from an actual large-n sample (He et al., 2019; Thomson et al., 2019). The peak date in this case would likely approximate the date of an "ideal" apatite, but a full accounting of the probability of various uncertainties would provide a more robust rationale for that interpretation.

Section 4.3. Timing of fragmentation

Finally, we emphasize that whether or not to apply the fragmentation correction in the first place is a decision that precedes the choice of the protocol. For non-detrital samples, any crystals with existing fractures prior to cooling would most likely still be intact, from an alpha-ejection perspective (i.e. the fragments are immediately adjacent, such that He is implanted across fractures). This means that the fragmentation correction to a crystal that has lost one or two termination(s) would still need to be applied even if a fracture was present before cooling. On the other hand, the question of when the fracture occurred matters for He diffusion. Depending on the thermal history, and whether the fracture pathway was a free surface for He loss, the He concentration profile of the fragment would be the result of some

combination of alpha ejection having acted on external non-fragmented surfaces and diffusion having acted on all free surfaces. An additional complication, for certain thermal histories (e.g. partially reset samples), is that a broken face that is still adjacent to the other broken side (so that it has not experienced alpha-ejection helium loss) may experience more diffusion at this fracture plane than the exposed external faces where diffusion is inhibited by the lower He concentration at the crystal boundary.

For detrital samples the situation is more complicated. The accuracy of the protocol proposed above, as with the previous fragmentation protocol, is founded upon the assumption that fragmentation occurred recently, relative to the timing of cooling. This is not always straightforward to assess. For samples such as modern river sands derived from crystalline rocks, an assumption that c-axis-perpendicular breakage occurred after cooling (approximately below the closure temperature) can be reasonably based on textural clues, particularly the contrast between detrital apatite grains that are rounded or abraded by transport and the sharp faces and corners of fragment surfaces that have not. For sedimentary samples that have not been clearly buried and reset, e.g. sedimentary rocks not buried more than couple km, the timing of fragmentation would be more ambiguous, unless the age of the deposition is known (assuming that the age of the deposition is close to the age of erosion and transport, and therefore the timing of fragmentation).

Analogous to problem of unknown timing of abrasion for rounded detrital apatite and zircon grains (Rahl et al., 2003; Thomson et al., 2013; Reiners et al., 2018), if the timing of fragmentation is unknown, we could define a maximum date A_{fc}, the F_T-corrected date without fragmentation correction, corresponding to fragmentation before or immediately after cooling; and a minimum date A_{ffc}, the fully FT-corrected date with fragmentation correction, corresponding to fragmentation during laboratory mineral separation. If there is sufficient geologic context, we can take the date of the sediment A_s to be the latest time at which the fragmentation occurred, such that the minimum date, A_{min}, would instead be:

$A_{min} = (A_{ffc}) + (A_{fc}-A_{ffc})(A_s/A_{fc})$

[Eq. 7]

A conservative approach would then be to display a "plot date" that is the mean of the maximum and minimum possible dates, and an error bar depicting the possible range of dates (Thomson et al., 2013).

In the case of detrital samples for which the timing of fragmentation is unknown, and that have also experienced non-monotonic cooling so that there has been significant diffusive loss after fragmentation (e.g. fragment in a sedimentary rock that has been partially reset by burial-induced heating), fragmentation-corrected dates will be systematically younger than the corrected dates of whole, unbroken grains. For example, the corrected dates of any whole crystal may reflect a date-Rs (sphere-equivalent radius) relationship, and naively applying the fragmentation correction to fragments will lead to corrected dates that all lie below this the corrected date-Rs relationship of unbroken crystals. In this case, a plot

435 date with a maximum and minimum date could still be calculated, as defined above. The plot dates would reflect a similar date-Rs relationship: i.e. if fragmentation occurred soon after cooling and significantly before partial reheating, the maximum date A_{fc} would be the closest to the corrected date of an equivalent unbroken grain (except that it would be younger than the equivalent unbroken grain to the extent that the unbroken grain is less affected by diffusion due to its size). To consider the date-size relationship of

440 fragments, it would be necessary to either calculate an assumed sphere-equivalent radius (Rs′) using the half-width and an assumed aspect ratio for typical ratios, or to use a sphere-equivalent radius based on F_T (cf. Cooperdock et al., 2019), using the fragment's alpha-ejection-affected-F_T value proposed here. The rationale for the latter option would be analogous to the case of the fragmentation F_T correction: the alpha-ejection-affected surface-to-volume ratio of a broken crystal is a good proxy for the available-for-

445 diffusion-surface-to-volume ratio.

In all cases where significant diffusive loss complicates the application of fragmentation correction, the best way to approach the problem may be to consider a combination of factors in deciding whether to apply the fragmentation correction or calculate a plot age that is combination of the fragment-corrected date and the normal F_T-corrected date: a.) whether the fragment-corrected dates are systematically

450 younger than the corrected dates of unbroken grains, b.) whether there is geologic context to suspect earlier fragmentation, and c.) whether there is a date-size correlation of corrected dates of unbroken grains.

5. Conclusion

455 Despite the dispersion of raw (U-Th)/He dates due to fragmentation, it is possible to accurately correct for the effect of fragmentation based on basic measurements routinely recorded during the grain selection process. In compensating for the effects of alpha ejection in broken crystals, the F_T correction should be calculated by explicitly taking into account the surface area of the broken face, rather than by assuming the unknown length of the original unbroken crystal. In individual cases, especially crystals with smaller

460 width or whose length is less than or around the same as the width, the difference in apparent dates calculated with the two methods can be 12% or greater.

We further applied both the previous and newly proposed protocol for correction of broken crystals to a synthetic dataset. Even taking into account the effects of diffusive loss of helium and breakage close to tips of crystals, the proposed protocol more accurately and more precisely approximates the F_T-corrected

465 date of an unbroken crystal for a range of complex and simple thermal histories. For a crystal of 150 μm width, the old calculation leads to apparent dates that are on average 3% older than the corrected dates of

unbroken crystals, and in extreme cases, up to 20% (e.g. for drum-shaped fragments with no terminations that experienced gradual reheating).

The proposed adjustment allows more accurate comparison of data between samples of varying quality, which is common when a mix of different rock types is sampled. The greatest effect will be for samples where the majority of crystals are broken. Though this adjustment is minor in many cases, when applied to entire datasets, it significantly reduces one common source of error in calculations of individual apparent dates, and removes an easily correctable source of systematic bias towards older dates.

Acknowledgment

We thank Richard Ketcham and an anonymous referee for their thorough and constructive reviews, and Stuart Thomson for the insightful discussions that led to this paper. JH acknowledges the support of H.W. and M.W. Peirce Scholarship and the ARCS Foundation Papadopoulos Fellowship. The analyses in this paper were in part built upon the innovative work of Roderick Brown, whose careful consideration of the problem of crystal fragments in He dating, among many others, made lasting contributions to the thermochronology community.

Code availability

Kernel density plots were produced using DensityPlotter (https://www.ucl.ac.uk/~ucfbpve/densityplotter/)

Data availability

Individual corrected fragment dates can be found in the supplementary file, and are calculated using methods discussed in text and applied to the cited synthetic datasets.

Author Contribution (CReDIT taxonomy)

JH – Conceptualization, formal analysis, methodology, visualization, writing-original draft; PWR-Supervision, resources, methodology, writing-review and editing

Competing Interests

The authors declare they have no competing interests.

References

Ault, A. K. and Flowers, R. M.: Is apatite U–Th zonation information necessary for accurate interpretation of apatite (U–Th)/He thermochronometry data?, Geochim. Cosmochim. Acta, 79, 60–78, https://doi.org/10.1016/j.gca.2011.11.037, 2012.

Beucher, R., Brown, R. W., Roper, S., Stuart, F., and Persano, C.: Natural age dispersion arising from the analysis of broken crystals: Part II. Practical application to apatite (U-Th)/He thermochronometry, Geochim. Cosmochim. Acta, 120, 395–416, https://doi.org/10.1016/j.gca.2013.05.042, 2013.

Brown, R. W., Beucher, R., Roper, S., Persano, C., Stuart, F., and Fitzgerald, P.: Natural age dispersion arising from the analysis of broken crystals. Part I: Theoretical basis and implications for the apatite (U-Th)/He thermochronometer, Geochim. Cosmochim. Acta, 122, 478–497, https://doi.org/10.1016/j.gca.2013.05.041, 2013.

Cooperdock, E. H. G., Ketcham, R. A., and Stockli, D. F.: Resolving the effects of 2D versus 3D grain measurements on (U-Th)/ He age data and reproducibility, Geochronol. Discuss., 1–32, https://doi.org/10.5194/gchron-2019-3, 2019.

Dana, E. s.: A Textbook on Mineralogy, John WIley, New York, 1963.

Farley, K. A.: (U-Th)/He Dating: Techniques, Calibrations, and Applications, Rev. Mineral. Geochemistry, 47, 819–844, https://doi.org/10.2138/rmg.2002.47.18, 2002.

Farley, K. A. and Stockli, D. F.: (U-Th)/ He Dating of Phosphates :, Rev. Mineral. Geochemistry, 15, 559–577, https://doi.org/10.2138/rmg.2002.48.15, 2002.

Farley, K. A., Wolf, R. A., and Silver, L. T.: The effects of long alpha-stopping distances on (U-Th)/He ages, Geochim. Cosmochim. Acta, 60, 4223–4229, https://doi.org/10.1016/S0016-7037(96)00193-7, 1996.

Farley, K. A., Shuster, D. L., and Ketcham, R. A.: U and Th zonation in apatite observed by laser ablation ICPMS, and implications for the (U-Th)/He system, Geochim. Cosmochim. Acta, 75, 4515–4530, https://doi.org/10.1016/j.gca.2011.05.020, 2011.

Fitzgerald, P. G., Baldwin, S. L., Webb, L. E., and O'Sullivan, P. B.: Interpretation of (U-Th)/He single grain ages from slowly cooled crustal terranes: A case study from the Transantarctic Mountains of

520 southern Victoria Land, Chem. Geol., 225, 91–120, https://doi.org/10.1016/j.chemgeo.2005.09.001, 2006.

Flowers, R. M., Ketcham, R. A., Shuster, D. L., and Farley, K. A.: Apatite (U-Th)/He thermochronometry using a radiation damage accumulation and annealing model, Geochim. Cosmochim. Acta, 73, 2347–2365, https://doi.org/10.1016/j.gca.2009.01.015, 2009.

525 Flowers, R. M., Zeitler, P. K., Danišík, M., Reiners, P. W., Gautheron, C., Ketcham, R. A., Metcalf, J. R., Stockli, D. F., Enkelmann, E., and Brown, R. W.: (U-Th)/He chronology: Part 1. Data, uncertainty, and reporting, Geol. Soc. Am. Bull., 2022a.

Flowers, R. M., Ketcham, R. A., Enkelmann, E., Gautheron, C., Reiners, P. W., Metcalf, J. R., Danišík, M., Stockli, D. F., and Brown, R. W.: (U-Th)/He chronology: Part 2. Considerations for evaluating, 530 integrating, and interpreting conventional individual aliquot data, Geol. Soc. Am. Bull., 2022b.

Gautheron, C., Tassan-Got, L., Ketcham, R. A., and Dobson, K. J.: Accounting for long alpha-particle stopping distances in (U-Th-Sm)/He geochronology: 3D modeling of diffusion, zoning, implantation, and abrasion, Geochim. Cosmochim. Acta, 96, 44–56, https://doi.org/10.1016/j.gca.2012.08.016, 2012.

He, J., Stuart N. Thomson, and Peter W. Reiners.: Apatite (U-Th)/He thermochronometric data show 535 rapid late Eocene incision in the central Transantarctic Mountains, AGU Fall Meeting Abstracts, vol. 2019, C53B-1340, https://ui.adsabs.harvard.edu/abs/2019AGUFM.C53B1340H/abstract, 2019.

He, J., Thomson, S. N., Reiners, P. W., Hemming, S. R., and Licht, K. J.: Rapid erosion of the central Transantarctic Mountains at the Eocene-Oligocene transition: Evidence from skewed (U-Th)/He date distributions near Beardmore Glacier, Earth Planet. Sci. Lett., 567, 117009, 540 https://doi.org/10.1016/j.epsl.2021.117009, 2021.

Herman, F., Braun, J., Senden, T. J., and Dunlap, W. J.: (U-Th)/He thermochronometry: Mapping 3D geometry using micro-X-ray tomography and solving the associated production-diffusion equation, Chem. Geol., 242, 126–136, https://doi.org/10.1016/j.chemgeo.2007.03.009, 2007.

Hourigan, J. K., Reiners, P. W., and Brandon, M. T.: U-Th zonation-dependent alpha-ejection in (U-545 Th)/He chronometry, Geochim. Cosmochim. Acta, 69, 3349–3365, https://doi.org/10.1016/j.gca.2005.01.024, 2005.

Ketcham, R. A., Gautheron, C., and Tassan-Got, L.: Accounting for long alpha-particle stopping distances in (U-Th-Sm)/He geochronology: Refinement of the baseline case, Geochim. Cosmochim. Acta, 75, 7779–7791, https://doi.org/10.1016/j.gca.2011.10.011, 2011.

550 Meesters, A. G. C. A. and Dunai, T. J.: Solving the production-diffusion equation for finite diffusion domains of various shapes: Part I. Implications for low-temperature (U-Th)/He thermochronology, Chem. Geol., 186, 333–344, 2002.

Murray, K. E., Orme, D. A., and Reiners, P. W.: Effects of U-Th-rich grain boundary phases on apatite helium ages, Chem. Geol., 390, 135–151, https://doi.org/10.1016/j.chemgeo.2014.09.023, 2014.

555 Palache, C., Clifford, F., and Berman, H.: The System of Mineralogy, John Wiley and Sons, 1963.

Rahl, J., Reiners, P. W., Campbell, I. H., Nicolescu, S., and Allen., C. M.: Combined single-grain (U-Th)/He and U/Pb dating of detrital zircons from the Navajo Sandstone, Utah." Geology 31.9 (2003): 761-764., Geology, 31, 761–764, 2003.

Reiners, P. W. and Farley, K. A.: Influence of crystal size on apatite (U–Th)/He thermochronology: an 560 example from the Bighorn Mountains, Wyoming, Earth Planet. Sci. Lett., 188, 413–420, https://doi.org/10.1016/S0012-821X(01)00341-7, 2001.

Reiners, P. W., Thomson, S. N., McPhillips, D., Donelick, R. A., and Roering, J. J.: Wildfire thermochronology and the fate and transport of apatite in hillslope and fluvial environments, J. Geophys. Res. Earth Surf., 112, https://doi.org/10.1029/2007JF000759, 2007.

565 Reiners, P. W., Carlson, R. W., Renne, P. R., Cooper, K. M., Granger, D. E., McLean, N. M., and Schoene, B.: Geochronology and Thermochronology, WIley, 2018.

Spiegel, C., Kohn, B., Belton, D., Berner, Z., and Gleadow, A.: Apatite (U-Th-Sm)/He thermochronology of rapidly cooled samples: The effect of He implantation, Earth Planet. Sci. Lett., 285, 105–114, https://doi.org/10.1016/j.epsl.2009.05.045, 2009.

570 Thomson, Stuart N., Peter W. Reiners, John He, Sidney R. Hemming, and Kathy Licht: New constraints on the pre-glacial and glacial uplift and incision history of the central Transantarctic Mountains using multiple low-temperature thermochronometers, AGU Fall Meeting Abstracts, Vol. 2019, C14B-04, https://ui.adsabs.harvard.edu/abs/2019AGUFM.C14B..04T/abstract, 2019.

Thomson, S. N., Reiners, P. W., Hemming, S. R., and Gehrels, G. E.: The contribution of glacial erosion 575 to shaping the hidden landscape of East Antarctica, Nat. Geosci., 6, 203–207, https://doi.org/10.1038/ngeo1722, 2013.

Whipp, D. M., Kellett, D. A., Coutand, I., and Ketcham, R. A.: Short communication: Modeling competing effects of cooling rate, grain size, and radiation damage in low-temperature 580 thermochronometers, 4, 143–152, https://doi.org/10.5194/gchron-4-143-2022, 2022.

Wolf, R. A., Farley, K. A., and Kass, D. M.: Modeling of the temperature sensitivity of the apatite (U-Th)/He thermochronometer, Chem. Geol., 148, 105–114, https://doi.org/10.1016/S0009-2541(98)00024-2, 1998.

585   Zeitler, P. K., Herczeg, A. L., McDougall, I., and Honda, M.: U-Th-He dating of apatite: A potential thermochronometer, Geochim. Cosmochim. Acta, 51, 2865–2868, https://doi.org/10.1016/0016-7037(87)90164-5, 1987.

Ziegler, J. F.: Helium: Stopping powers and ranges in all elemental matter., 4, 1977.